Photoluminescence and Transient Spectroscopy of Free Base Porphyrin Aggregates

R. F. Khairutdinov

Institute of Chemical Physics, Russian Academy of Sciences, ul. Kosygina 4, 117334 Moscow, Russia

N. Serpone*

Center for Picosecond Laser Spectroscopy, Department of Chemistry and Biochemistry, Concordia University, Montreal, Quebec, Canada H3G 1M8

Received: January 23, 1998; In Final Form: November 9, 1998

Solutions of free base *meso*-tetraphenylporphyrin (H_2TPP), *meso*-tetra(4-carboxyphenyl)porphyrin (H_2TPPC), and *meso*-tetra(4-pyridyl)porphyrin (H_2TPyP) under various conditions generate aggregates whose absorption spectra are characterized by invariant Soret bands with bandwidths that are independent of the preparative method. One of the Soret bands is blue-shifted (H-aggregate) relative to the monomeric porphyrin band; other Soret bands are red-shifted (J-aggregates). The aggregates are characterized by different nonradiative rate constants for excited singlet-state decay and by different efficiencies of singlet−singlet annihilation at the high energies of laser excitation. The quantum yields of fluorescence vary between 10^{-5} and 10^{-2}, and the corresponding fluorescence lifetimes vary in the range from 10^{-12} to 10^{-9} s; they are more than 1 order of magnitude smaller than those of the corresponding monomeric porphyrins. Lifetimes (τ) correlate with the characteristic ground-state absorption recovery times of the aggregates. The sizes of the H-aggregate and aggregates that are characterized by a minimal blue shift of the Soret band range from 15 to 27 Å.

Introduction

Molecular aggregates (or clusters) play an important role in nature and in technological processes. Aggregates of chlorophyll molecules firmly held together in a unique spatial arrangement by specific neighboring proteins are responsible for the light harvesting and electronic energy transport to the reaction center of photosynthesis organisms, thereby leading to the high efficiency of natural photosynthesis.[1] Porphyrin molecular aggregates play an important role in photodynamic cancer therapy.[2−4]

The ability of chlorophylls, porphyrins, cyanine dyes, and other such compounds to form molecular aggregates in solution is well established.[5−7] Molecular aggregation of pigments can lead to blue- or red-shifted absorption bands and to the broadening of Soret and Q-bands; in other cases, narrowing of the Soret band may occur on aggregation.[8] Molecular aggregation of chlorophylls, porphyrins, and their structural analogues (the phthalocyanines) has been examined extensively by time-resolved spectroscopy, a direct and sensitive technique.[4,7,9−15] Typically, fluorescence quantum yields decrease on pigment aggregation. By contrast, the fluorescence quantum yield of bacteriochlorophyll *c* increases on aggregation.[16] Various forms of aggregates (face-to-face dimers, cyclic arrangement of three dimers, and H- and J-aggregates) have been inferred in interpreting optical absorption spectral changes and variations in fluorescence quantum yields of pigments in solution.[8,16−22] Emission lifetimes (τ) of concentrated chlorophyll solutions are about 3 orders of magnitude smaller than those of monomeric chlorophylls because of energy transfer and exciton migration within the chlorophyll aggregates.[10,23,24] Differences in fluorescence relaxation times of concentrated solutions of hematoporphyrin and tetraphenylporphyrin derivatives (τ 10 ps to 10 ns) have inferred the coexistence of dye aggregates, dimers, and monomers.[4,14,25−28] In general, the fast fluorescence decay in concentrated porphyrin solutions results from a sequence of strong intermolecular interactions within the aggregates. In the amorphous solid state, Hall and co-workers[29] reported the lifetime of the excited singlet in a tetraphenylporphyrin solid film, H_2TPP, to be ∼310 ps; by comparison, the fluorescence lifetime of the H_2TPP monomer in solution is ∼10 ns.[30]

The behavior of chlorophyll molecules linked together in complex structures in photosynthetic membranes also differs from that of an isolated pigment molecule. The emission quantum yield of a photosynthetic antenna system decreases at high laser fluence. Short, intense pulses used to probe fluorescence decay typically lead to multiexponential decay profiles with anomalously short lifetimes.[31,32] In single-pulse experiments, singlet−singlet annihilation of excited chlorophyll molecules in photosynthetic antennae systems, where several chlorophyll molecules may be coupled by excitonic interactions, accounts for the decrease in the emission probability.[33] Bimolecular singlet−singlet annihilation is a well-known phenomenon occurring when two or more singlet excitations appear simultaneously within the same spatial domain.[31,34−36] Such annihilation arises from dipolar interactions between two excited pigment molecules that induce a nonradiative transition in which one of the excited molecules relaxes to the ground state and the other is excited to a higher-energy state. Subsequently, the latter excited state rapidly returns to the lowest excited state, thus annihilating one of the two original excitations.

Aggregation of dye molecules adsorbed on silver halide grains provides the photographic film's sensitivity to visible and infrared light. In photography, dye aggregates play the role of light harvesters; electron−hole pair generation in the aggregate and subsequent electron transfer to the silver halide grains are the basic sensitization processes of photographic films.[37]

10.1021/jp980869s CCC: $18.00
Published on Web 01/15/1999

Molecular aggregates also display significant nonlinear optical responses and could prove of great importance in the field of integrated optics. Linear and nonlinear optical responses of molecular aggregates have recently been examined.[37−41] Aggregates consisting of several hundred molecules might have unusual properties, intermediate between single molecules and the bulk material.[42]

Interest in the theory of excitonic interactions in photosynthetic systems and the important role that porphyrin molecular aggregates play in cancer photodynamic therapy render a study of porphyrin aggregation an appealing subject, especially in instances where their behavior under light excitation depends on the structure of the multimolecular assemblies. Recent utilization[43] of physisorbed or chemisorbed inorganic dye antennae to sensitize wide band-gap semiconductors for light energy harvesting and conversion to a photoelectrochemical potential in a photoelectrochemical device, in which dye aggregation should not be precluded, also begs for added information on the photophysical events of molecular aggregation.

Little is known about the number of different types of porphyrin aggregates in solution together with their absorption and relaxation characteristics. Following our earlier work[44] on light attenuation in solutions of porphyrin aggregates, herein we report the photoluminescence and transient absorption features of porphyrin aggregates in solutions under high laser fluence. Under our experimental conditions, we describe four different types of aggregates[45] for the free base species examined that differ in their time-resolved absorption and fluorescence decay characteristics. Differences in these characteristics are likely due to differences in aggregate structures, the details of which remain elusive.

Experimental Section

meso-Tetraphenylporphyrin, H_2TPP, *meso*-tetra(4-carboxyphenyl)porphyrin, H_2TPPC, and *meso*-tetra(4-pyridyl)porphyrin, H_2TPyP, were all purchased from Strem Chemicals, Inc. Methanol, methyl ethyl ketone, MEK (Baker, reagent grade), hydrochloric acid, and NaOH (Aldrich, purest grade) were used without further treatment. The pH of the solution was adjusted either with HCl or NaOH. The water used for the preparation of all solutions was deionized and doubly distilled from a quartz still.

H_2TPP aggregate solutions were prepared by injecting a small volume of the porphyrin (0.5 mL or less) dissolved in MEK into water (2.5−3.0 mL). Aggregate solutions of H_2TPPC and H_2TPyP were prepared by mixing aqueous solutions of H_2TPPC (pH $\approx$ 10) or H_2TPyP (pH $\approx$ 3.5) with either acidic or alkaline water so that the resulting solution pH was either 3.5 or 10 for H_2TPPC and H_2TPyP, respectively. Typical porphyrin monomer concentrations in the aggregate solutions ranged from 10^{-6} to 10^{-5} M.

Absorption spectra were recorded with a Shimadzu UV-265 UV−vis spectrophotometer. Fluorescence experiments were carried out on a Perkin-Elmer MPF 44B spectrofluorimeter; excitation and emission slit widths were 3 nm. Solutions of low optical density (0.05 or less at the wavelengths of excitation) were used. The relative fluorescence quantum yields of aggregated porphyrins were determined by comparing the integrated fluorescence spectra per photon absorbed to those of the corresponding monomeric porphyrins on excitation in the appropriate Q-bands. In determining the relative fluorescence yields of aggregated porphyrins at different wavelengths, the relative number of absorbed photons was taken to be the integral of the product of the optical density and the relative photon intensity of the light source integrated over the band pass of the excitation monochromator slit. A solution of rhodamine B in ethylene glycol was the standard in the absolute fluorescence quantum yield measurements; accuracy was about ±10%.

Picosecond laser absorption spectroscopy experiments employed a frequency-tripled (355-nm pulses; fwhm $\approx$ 30 ps; average energy per pulse $\approx$ 2.5 mJ) double-beam and passively mode-locked Nd:YAG laser system, coupled to a fast detection unit that comprised a SIT (silicon intensified target) vidicon and an EG&G optical multichannel analyzer (OMA 3) coupled to an IBM 486DX computer. The probe pulse was a continuum generated from the 1064-nm fundamental by superbroadening in D_3PO_4 to give a wavelength range of approximately 400−700 nm. The absorption spectra were recorded by reading the intensities of a split probe pulse to obtain I_t $(1 - I_{abs})$ and I_o light intensities for attenuation calculation. The spectra at designated delay times after excitation at 355 nm are the averages of about 6−10 pairs of laser pulses. The solutions were stirred after each pulse to probe a different sample of the solution. Other descriptive details of the picosecond laser system may be found elsewhere.[46−48]

Time-resolved emission decay data were obtained by the streak camera method[49] using 355-nm pulsed laser excitation (fwhm $\approx$ 30 ps, average energy per pulse $\approx$ 2.5 mJ) and a Hamamatsu C979 streak camera; samples were prepared to yield optical densities of ~0.1 at this wavelength in a 2-mm cell. A laser-beam splitter diverted 10% of the pulse to an energy meter (Laser Precision Corp.), while the remaining light was smoothly focused onto a 4 mm^2 area of the 2 mm path length quartz cuvette. The fluorescence was collected from the front surface and collimated by a 50 mm diameter lens (f/1.5). A second lens (focal length $\approx$ 60 mm; f/1.2) focused collected light through a 100 μm slit of the streak camera onto a red-sensitive multialkali photocathode. Polarization of the fluorescence was detected using a polarizing filter immediately in front of the photomultiplier tube. Parallel and perpendicular orientations of the filter with respect to the orientation of the exciting light were used in these experiments. The streak camera was protected with a 400-nm cutoff UG-11 filter to prevent detection of scattered and Raman-shifted pump radiation.

All experiments were carried out at ambient temperature with freshly prepared air-equilibrated solutions.

Deconvolution of the multicomponent absorption spectra of the solutions of aggregates was performed using the program PeakFit v4.00 for Win32 (Jandel Scientific Software). A Gaussian shape of the spectral bands of the individual components was assumed in the calculations.[50]

Results and Discussion

Absorption Spectra. H_2TPP is a hydrophobic free base porphyrin soluble in organic solvents; H_2TPPC and H_2TPyP are water-soluble pigments at basic and acidic pH, respectively. Absorption spectra of the monomeric forms of these porphyrins are characterized by a Soret absorption in the blue end of the visible region ($\epsilon > 10^5$ M^{-1} cm^{-1}) and by four Q-bands located in the 500−600 nm region ($\epsilon \leq 10^4$ M^{-1} cm^{-1}). Absorption band maxima of monomeric porphyrins in MEK (H_2TPP) and in water at pH 10 (H_2TPPC) and at pH 3.5 (H_2TPyP) are summarized in Table 1.

Injection of MEK solutions of monomeric H_2TPP into water or a change in pH of the H_2TPPC or H_2TPyP monomeric

TABLE 1: Soret and Q-Band Maxima of Monomeric and Aggregated Forms of Free Base Porphyrins[a]

porphyrin	adsorption band maxima, nm[b]									
	monomeric form					aggregated form				
	Soret	Q1	Q2	Q3	Q4	Soret	Q1	Q2	Q3	Q4
H_2TPP	413(12)[c]	512	534	588	645	(1) 392(75) (2) 423(55) (3) 451(20) (4) 470(57)	522	546	594	650
H_2TPyP	413(24)	515	551	582	640	(1) 396(63) (2) 434(38) (3) 443(11) (4) 469(33)	518	550	590	643
H_2TPPC	414(12)	518	555	580	635	(1) 392(70) (2) 425(53) (3) 442(31) (4) 460(69)	522	559	595	651

[a] For the free base porphyrin aggregates, the positions of the maxima of the individual components are presented. [b] Accuracy in the absorption maxima and in the bandwidths is about ±1 nm. [c] Values in brackets are the bandwidths at half-height (nm).

solutions in water to pH 3.5 or 10, respectively, yields distinct changes in the absorption spectra: (i) the Soret band feature is considerably broader and consists, in part, of several red-shifted bands, (ii) Q-bands are also red-shifted but to a lesser extent. These changes point to aggregation of porphyrin molecules in solutions.[6,7,51] We ascribe the different components in the Soret absorption band region to different porphyrin aggregates which are characterized by different geometric arrangements of the chromophores.[8] By contrast, slow (drop by drop) addition of water to monomeric solutions of H_2TPP generates large porphyrin aggregates, as evidenced by solution turbidity and absorption spectra exhibiting nonhorizontal baselines.

H_2TPP Aggregate Solutions. For the H_2TPP aggregate system, the Soret absorption feature consists of several components for which the relative intensities depend on the initial concentration of the monomeric solutions. Typically, injection of a low-concentration MEK porphyrin solution into water yields relatively intense absorption at short wavelength in the Soret band region (porphyrin concentration $\leq 10^{-5}$ M). At higher concentrations of monomer solution, the long-wavelength portion of the Soret band becomes increasingly more intense. The shapes of the Q-bands of the aggregated porphyrins are independent of the porphyrin monomer concentration.

The time evolution of the Soret spectral feature of aggregate solutions prepared from a low concentration of the monomeric porphyrin ($\leq 10^{-5}$ M) is illustrated in Figure 1a for H_2TPP. At short times, the decrease in intensity of the shorter wavelength shoulder is accompanied by an increase of the absorption at the longer wavelength. A clean isosbestic behavior (ca. 450 nm) is characteristic of this transformation in the first 25 min. At longer times (~10 h), all the porphyrin absorption bands have decreased in intensity owing to aggregate precipitation.

Solutions of aggregates prepared from more concentrated monomeric porphyrin solutions ($\geq 10^{-4}$ M) show only small temporal changes in the shape and peak intensity of the absorption spectra in the interval 400−450 nm over the first 2 h after preparations (Figure 1b; the inset illustrates the absorbance decay at different wavelengths).

In all cases, simple Gaussian deconvolution of the Soret absorption spectral region gave four individual components.[45] The positions and bandwidths of the components are independent of the initial concentrations of the monomeric porphyrin solutions (10^{-5} to 10^{-4} M); only the relative intensities of the components varied with changes in the initial concentrations of the monomers. Spectral maxima and bandwidths (at half-height) of these components that yield the best fit to the experimental absorption spectra of aggregates in the Soret region are summarized in Table 1.

Figure 2 illustrates an example of the deconvolution of the absorption spectrum (data points) of the aggregate solution prepared from high (10^{-4} M) concentrations of monomeric H_2TPP. Dashed lines represent the four individual components, the sum of which gives the spectrum shown by the solid lines.

H_2TPPC and H_2TPyP Aggregate Solutions. For these water-soluble porphyrins, aggregation caused by pH changes leads to a broad multicomponent Soret absorption band. Aggregation in aqueous solutions occurs even for the H_2TPPC porphyrin that carries four negative charges on the periphery of the molecule as do many other charged dyes.[52−54] Electrostatic repulsion between dye molecules is reduced by delocalization of the charge over the aromatic ring system.[55]

Absorption spectra of H_2TPPC and H_2TPyP aggregates in the Soret band region were also resolved into four individual components for the best fit. The positions and bandwidths of these individual components remain unchanged (Table 1) in the porphyrin concentration range 10^{-5} to 10^{-6} M.

Origin of the Individual Components in the Soret Band of Porphyrin Aggregates. Different components in the Soret absorption bands of solutions of aggregates are likely to coincide with porphyrin aggregates that possess different geometrical arrangements of the chromophores.[8] An isosbestic point, characteristic of the spectral changes at low porphyrin concentration (see e.g. Figure 1a), indicates that at least two different types of aggregates exist in the porphyrin solutions. They are indicated in Table 1 as 2 and 3. We infer that the two additional Soret components correspond to two other aggregates since the relative intensities of all four individual components depend on the initial porphyrin concentration. In this regard, H- and J-aggregates are known to be produced on aggregation of dyes in solutions. Porphyrin dimers (and trimers) in which two (or three) porphyrin cores are chemically connected by molecular bridges show a blue-shifted Soret band upon dimerization (or trimerization).[56,57] A broadened red-shifted Soret band has been observed in long-range stacked structures produced by *cis*- and *trans-meso*-diphenylbis(*N*-methyl-4-pyridyl)porphyrin associated to DNA.[58]

Kasha's analysis of energy relaxation from excited states of molecular aggregates[59] predicts that a stacked face-to-face π-aggregation (sandwich-type H-aggregate) leads to a spectral blue shift relative to the monomer excited-state level, whereas the corresponding spectral feature from a tilted "deck of cards" (J-aggregate) aggregation leads to a red shift. The extent of this $\pi \rightarrow \pi^*$ band shift depends on (i) the degree of aggregation, (ii) the interplanar separation distance, (iii) the mutual orientation of the monomers in the aggregate including the tilt angle with the molecular stack, (iv) electronic transition probabilities, and (v) the specific sensitivities of the chromophore.[57,60−62] Intermolecular electronic interactions within the aggregates cause the degeneracy in the excited-state electronic energy levels to be lifted. Thus, an orbitally allowed transition between the lowest (unsplit) ground state and the antibonding excited-state levels results in blue-shifted absorption in H-aggregates. For J-aggregates, transitions to the lower energy excited state are allowed, resulting in the red shift of their absorption band(s). For porphyrins containing phenyl groups, an additional red shift of the absorption may occur because of enhanced coplanarity between the porphyrin core and the phenyl rings (enhanced

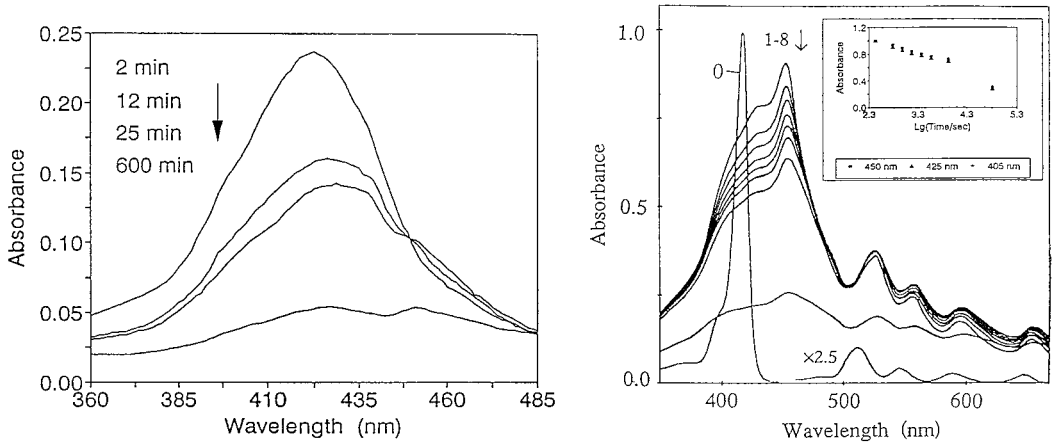

Figure 1. H_2TPP absorption spectra at different times after injection of a MEK porphyrin solution to water (1/10, v/v); concentration of the porphyrin in MEK is (a) 10^{-5} M and (b) 10^{-4} M. Spectrum 0: H_2TPP spectrum in MEK (2.3×10^{-6} M). Spectra 1−8: H_2TPP spectra after 4, 10, 15, 27, 40, 60, and 130 min and 16 h after injection. The inset in b shows the kinetics of the absorption decrease after injection at different wavelengths.

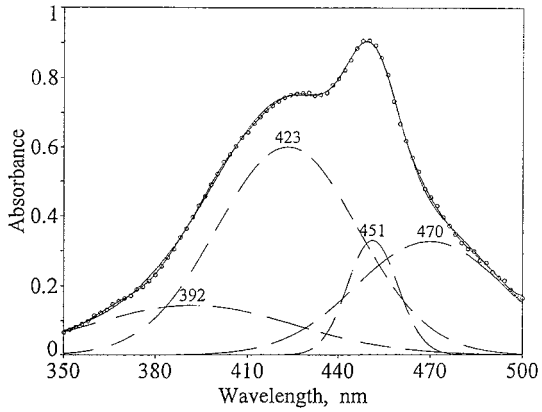

Figure 2. H_2TPP absorption spectra after 2 min following injection of a MEK porphyrin solution to water (1/10 v/v) (points). Dashed lines show the individual components, the sum of which (solid lines) gives the best fit to the experimental absorption spectra of the aggregate solution. The concentration of the porphyrin in MEK is 10^{-4} M.

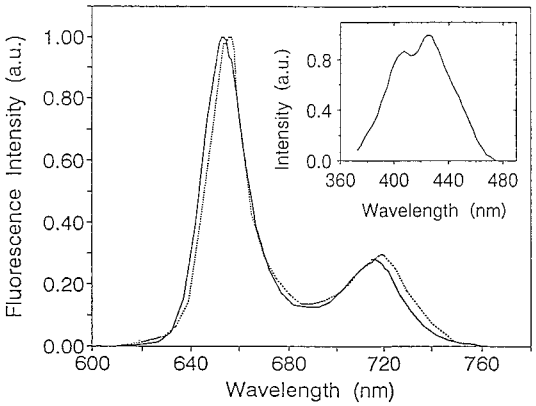

Figure 3. Normalized fluorescence spectra of monomeric (solid line) and aggregated (dashed line) H_2TPP solutions; excitation wavelength, 517 nm; aggregate solutions prepared from an MEK solution 10^{-4} M in H_2TPP. Excitation spectrum of aggregated H_2TPP solution is shown in the insert ($\lambda_{em} = 656$ nm).

conjugation of phenyl rings to the porphyrin core) within the J-aggregates, a result of molecular packing constraints.[8]

Different types of premicellar H- and J-aggregates are obtained in dilute aqueous surfactant solutions of several picket-fence porphyrins.[8] Some porphyrins display very narrow, red-shifted Soret bands (narrower than the Soret band of the porphyrin monomers) that are typical of dye J-aggregates, whereas broad Soret absorptions have been observed in others. A broad Soret band originates from a multiplicity of excitonic J-aggregate interactions arising from a variety of interplanar porphyrin−porphyrin core geometries. The structure of a porphyrin aggregate and, hence, the position and the width of the Soret band depend on the nature of the solvent. For example, addition of alcohol or surfactants to disordered aqueous aggregates leads to a modest reorganization of the porphyrin chromophores.

On the basis of the above considerations, our data are consistent with the formation of various J-aggregates containing three or more porphyrin monomers in aqueous solutions of the porphyrins, insofar as the large shifts of the Soret band and the multicomponent structure of the absorption indicate that the observed spectra cannot be attributed solely to a solvent effect. Also, to the extent that the degree of exciton coupling in an aggregate is related to the number of interacting chromophores, N, the degree of $\pi \rightarrow \pi^*$ character in the absorption band shift, $\Delta\nu_{abs}$, should increase with an increase in N under otherwise constant interaction parameters.[63] Accordingly, the shift of the excitonic band when $N = 2$ will be 2-fold smaller than that in infinite aggregates of identical geometry. Note that the excited state of the J-aggregate is a neutral excitonic state.

Fluorescence Spectra. Fluorescence spectra of monomeric and aggregated porphyrins consist of two emission bands characteristic of this class of pigments.[64] The two-band red-shifted luminescence observed in porphyrin solutions examined here is typical of J (and H) porphyrin aggregates. One such example is illustrated in Figure 3, which shows the normalized fluorescence spectra of monomers (solid line) and aggregates (dashed line) in H_2TPP solutions. Neither the position nor the relative intensities of the aggregate emission bands depend on the method of aggregate preparation for low, $\leq 10^{-5}$ M, or high, $\geq 10^{-4}$ M, concentrations of monomeric porphyrins before aggregation. The positions of the fluorescence band maxima of the monomeric and aggregated porphyrins are collected in Table 2.

The magnitude of the red shifts of the fluorescence band is reasonable for the porphyrins examined. Excitation spectra of all porphyrin aggregates correlate with their corresponding absorption spectra (see, e.g., insert in Figure 3 and compare with absorption spectrum in Figure 2).

Fluorescence quantum yields of the porphyrins examined in the monomeric state, ϕ_o, range between 0.03 and 0.10, larger than the emission quantum yields of porphyrin aggregate

TABLE 2: Wavelengths of the First Fluorescence Maximum and Quantum Yields of Free Base Porphyrin Monomers (λ^o_{max}, ϕ_o,) and Aggregates (λ_{max}, ϕ), and Calculated Values of the Quantum Yields (ϕ_i) and Emission Lifetimes (τ_i) of Individual Aggregates

porphyrin	λ^o_{max}, nm[a]	λ_{max}, nm[a]	ϕ_o[b]	10^2 ϕ[c]	no.	10^2 ϕ_i[b]	τ_i, ps[d]
					1	0.27	280
					2	0.15	156
H_2TPP	653	656	0.10	0.36	3	(0.7)[e]	(700)[e]
					4	0.003	3.1
					1	0.15	184
					2	0.12	147
H_2TPyP	660	662	0.08	0.19	3	(0.6)[e]	(700)[e]
					4	0.004	4.8
					1	0.019	24
					2	0.024	30
H_2TPPC	648	675	0.09	0.036	3	(0.2)[e]	(250)[e]
					4	0.001	1.2

[a] Accuracy of the fluorescence maxima values is about ±1 nm. [b] Accuracy of the quantum yield values is about ±10%. [c] Excitation in the Q1-band; accuracy of quantum yield values about ±10%. [d] Accuracy in the lifetime values is about ±20%. [e] Estimate (see text for more detail).

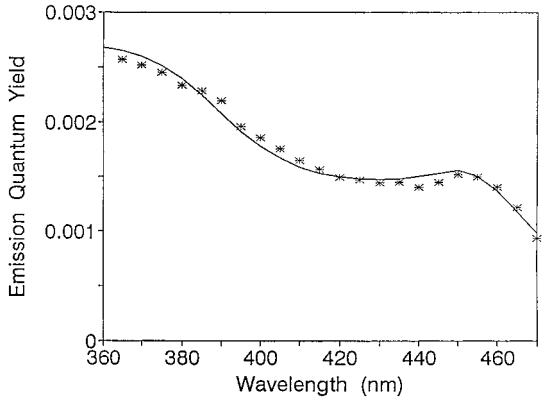

Figure 4. Wavelength dependence of the emission quantum yields of a solution of H_2TPP aggregates; λ_{em} = 656 nm. Points: experimental data. Curve: the best fit of the experimental data with the help of eq 1 (see text).

solutions, ϕ, under excitation of the Q1-band (Table 2). These solutions are characterized by a wavelength-dependent emission efficiency on excitation in the wavelength range from 360 to 470 nm (Figure 4) for the fluorescence quantum yield of an H_2TPP aggregate solution with λ_{em} = 656 nm. This wavelength dependence of ϕ of the aggregates mirrors the difference in the emission quantum yields of the different aggregates. Denoting ϕ_i as the quantum yield of the *i*th aggregate in the cluster of aggregates, the total quantum yield of the solution is given by (eq 1)

$$\Phi_\lambda = \frac{A_1(\lambda)\phi_1 + A_2(\lambda)\phi_2 + A_3(\lambda)\phi_3 + A_4(\lambda)\phi_4}{A_1(\lambda) + A_2(\lambda) + A_3(\lambda) + A_4(\lambda)} \quad (1)$$

where $A_i(\lambda)$ is the absorption profile at different wavelengths of the *i*th aggregate. The respective quantum yields ϕ_i of the different aggregates were obtained from an analysis (eq 1) of the experimental data on the wavelength dependence of the emission quantum yield of porphyrin solutions; they are collected in Table 2. These ϕ_i values gave the best fit (solid line) of the experimental data depicted in Figure 4 for an H_2TPP solution. Only an estimate of ϕ_3 is given because of the low relative concentrations of aggregate **3** in dilute porphyrin solutions used in the experiments for quantum yield determinations. Table 2 also shows that the emission quantum yields of aggregates **1**, **2**, and **3** strongly exeed ϕ_4 of aggregate **4**. The fluorescence lifetime, τ_i, for each individual aggregate was evaluated from the expression $\tau_i = \tau_o\phi_i/\phi_o$ (see below) and from the emission quantum yields ϕ_o of monomeric porphyrins (Table 2); the corresponding fluorescence lifetimes, τ_o, are summarized in Table 3.

TABLE 3. Characteristic Times of Transient Absorption Decay and Fluorescence Decay of Porphyrin Solutions[a]

porphyrin	τ_o, ns	τ, ps	τ'_2, ps	τ'_3, ps	τ_r, ps
H_2TPP[b]	10.4 ± 0.5	187 ± 13	250 ± 75	1000 ± 300	110 ± 15
H_2TPyP	9.8 ± 0.5	96 ± 10	150 ± 45	700 ± 200	190 ± 25
H_2TPPC	11.3 ± 0.6	35 ± 10	100 ± 30	500 ± 150	87 ± 15

[a] τ_o = fluorescence lifetime of porphyrin monomers; τ = characteristic time of porphyrin aggregates fluorescence decay; τ'_2 and τ'_3 = the transient absorption decay times for aggregates **2** and **3** (Table 1), respectively; τ_r = rotational relaxation time of aggregates. [b] Aggregates were prepared by injection of a highly concentrated porphyrin solution to water (see text).

Time-Resolved Absorption Spectra. *Monomeric Porphyrins.* Pulsed laser excitation of monomeric metalloporphyrin solutions typically results in the bleaching of the porphyrin absorption band and in the appearance of a broad absorption centered around 450 nm.[65] The Soret band of free base porphyrins is positioned at wavelengths below the spectral range of 425−675 nm available to our laser system, and therefore, solutions of monomeric free base porphyrins were not examined.

Porphyrin Aggregates. Transient spectra of porphyrin aggregates were monitored between 425 and 675 nm. Our experimental conditions precluded examination of the transient behavior of any aggregate having a Soret band component at $\lambda_{max} \ll 420$ nm: e.g., aggregates **1** of H_2TPP and H_2TPyP or aggregates **1** and **2** of H_2TPPC (Table 1). Aggregates that display strong absorption around 425−450 nm showed a pulse-width-limited (≤30 ps) bleaching of the aggregates Soret absorption followed by absorption recovery at longer delay times. We observed no absorption bleaching in aggregates having long-wavelength Soret bands ($\lambda_{max} > 460$). For the porphyrins examined here, aggregate **4** contributes significantly to the absorption spectra of the solution in this wavelength region. Hence, the absence of bleaching at $\lambda_{max} > 460$ nm infers that the characteristic recovery time of aggregates **4** is also pulse-width-limited. In this context, it is worth noting that strong light attenuation occurs in the nanosecond time scale, which originates from scattering of the analyzing light by temperature inhomogeneities produced by the laser pulse excitation in aggregate solutions (for a recent detailed account of this phenomenon, see ref 44).

In all the porphyrins examined, changes in transient absorption at the shorter wavelengths of the Soret band region occur faster than those at the longer wavelengths; compare, for example, the transient absorption changes at 425 and 450 nm of the H_2TPP and H_2TPPC aggregates (Figure 5a and 5b). The faster recovery of the short-wavelength wing of the transient absorption alters the shape of the spectra such that only bleaching of the pronounced band centered at the same wavelength(s) as the Soret absorption maximum of aggregates **3** (see Table 1) is observed at the longer delay times. For the case of H_2TPPC, the transient absorption spectrum (Figure 5b) was deconvoluted by subtraction of the spectrum obtained at 0 ps from that recorded at a 150 ps delay to leave a distribution of absorption identical to the red "component" of the ground-state absorption spectrum assigned to aggregate **2**. This result is consistent with the absorption spectral analysis and shows

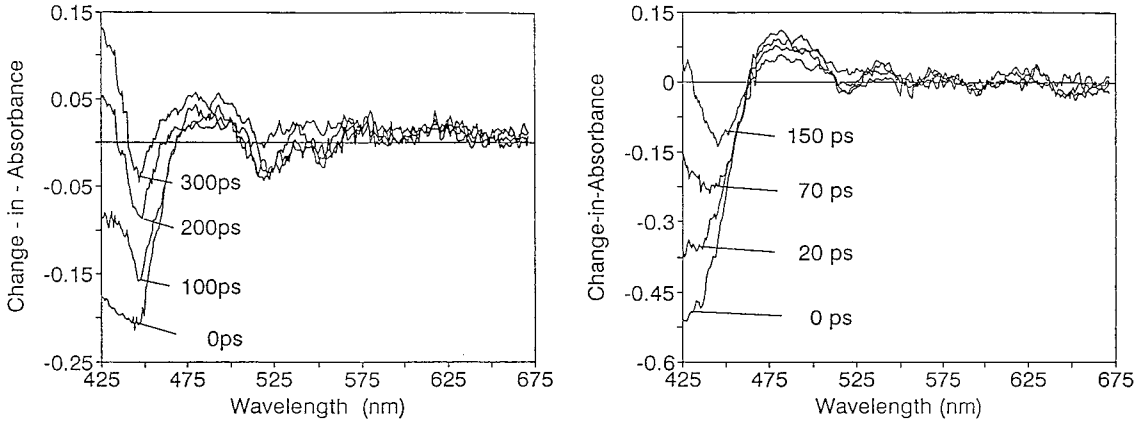

Figure 5. Transient absorption spectra of excited aggregates of (a) H_2TPP and (b) H_2TPPC solutions at different times after the 30-ps laser pulse; H_2TPP aggregate solutions were prepared from a 10^{-4} M H_2TPP solution in MEK.

that absorption recovery of each of the different porphyrin aggregates takes place at different rates.

The transient absorption changes were quantitatively characterized at several wavelengths between 425 and 450 nm on the basis that only aggregates **2** and **3** are responsible for these changes and that recovery of each type of aggregate absorption is governed by an exponential law. Consequently, the temporal changes can be described by (eq 2)

$$\Delta A^{\lambda} = \Delta A_2^{\lambda}(0)\exp\{-t/\tau'_2\} + \Delta A_3^{\lambda}(0)\exp\{-t/\tau'_3\} \quad (2)$$

where ΔA^{λ} is the change in the sample absorbance at wavelength λ and $\Delta A_2^{\lambda}(0)$ and $\Delta A_3^{\lambda}(0)$ are the time-independent constants, whereas τ'_2 and τ'_3 are the characteristic recovery times of the absorption bands of aggregates **2** and **3**, respectively (Table 3).

Typical kinetics of transient absorption changes at 425 and 450 nm are presented in Figure 6a and 6b (points). The solid lines on these figures were drawn using eq 2 and appropriate values of $\Delta A_2^{\lambda}(0)$ and $\Delta A_3^{\lambda}(0)$ and of τ'_2 and τ'_3: ~250 ps and 1 ns for H_2TPP and ~100 and 500 ps for H_2TPPC, respectively. These absorption recovery times mirror the fluorescence lifetimes τ_2 and τ_3 obtained from emission quantum yield data (Table 2); the pulse-width-limited recovery times for aggregates **4** correlate with the corresponding low emission lifetimes τ_4 (<10 ps, Table 2).

Fluorescence Decay Kinetics. Fluorescence decay kinetics of solutions of monomeric porphyrins follow an exponential law with lifetimes, τ_o, of the order of several nanoseconds (Table 3), in good accord with those reported earlier.[66] The emission decay of porphyrin aggregates remains exponential but is about 2 orders of magnitude faster than the emission decay of monomeric porphyrin molecules. Typical fluorescence decay kinetics of such aggregates are shown in Figure 7 for the H_2TPP system. The solid curve was drawn using the expression $I(t) \propto \exp(-t/\tau)$; emission lifetimes τ are summarized in Table 3.

The emission decay envelope illustrated in Figure 7 comprises the emission decays of the different types of aggregates in the solutions. As noted in Table 2, the emission lifetimes of aggregates **1** and **2** (τ_1 and τ_2) estimated from the quantum yield values concur with τ whereas the emission lifetimes of aggregates **3** and **4** differ considerably from the fluorescence decay lifetimes τ. We ascribe this variation to the dominance of the fluorescence decay of aggregates **1** and/or **2** on the observed emission decay kinetics.

The quantum yield of fluorescence is related to the radiative rate constant, k_r, and to the lifetime of deactivation of the excited

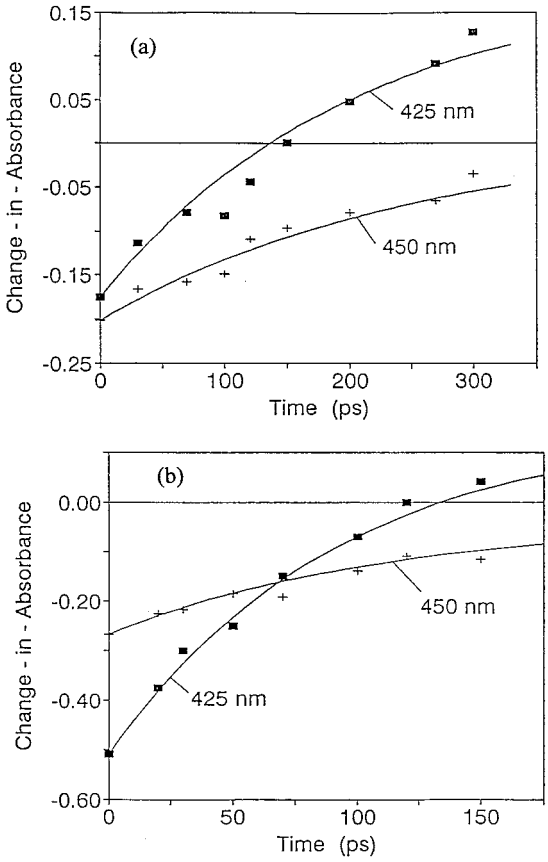

Figure 6. Kinetics of transient absorbance changes of (a) H_2TPP and (b) H_2TPPC aggregates at two different wavelengths. Points: experimental data. Lines: results of the calculations from eq 2 using values of τ'_2 and τ'_3 from Table 1 and appropriate values of $\Delta A_2^{\lambda}(0)$ and $\Delta A_3^{\lambda}(0)$.

state, τ, by (eq 3)

$$\phi_i = k_r\tau \quad (3)$$

where

$$\tau^{-1} = k_r + k_{nr} \quad (4)$$

and k_{nr} denotes the sum of all the nonradiative excited singlet-state decay channels, e.g., intersystem crossing and internal conversion.

The radiative rate constant k_r does not seem to vary significantly on aggregation since few, if any, changes take place

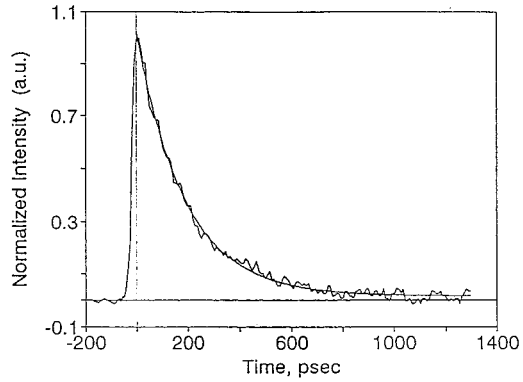

Figure 7. H_2TPP emission decay after laser excitation. Smooth curve, result of the experimental data fitting by an exponential decay law with $\tau = 187$ ps.

in the Q_x absorption bands of the aggregates. The oscillator strength of these Q_x bands is very similar to that of the Q_x bands of monomeric porphyrins. It appears then that aggregation enhances the rate of nonradiative transitions in porphyrin molecules. Consequently, differences between the fluorescence decay lifetimes of different aggregates largely reflect differences in the nonradiative rate constants for excited singlet-state decay. The k_{nr} of porphyrins monomers and aggregates, evaluated from eqs 3 and 4 and with the aid of emission quantum yields and emission lifetimes from Tables 2 and 3, are summarized in Table 4.

Aggregates **4** are characterized by very small decay times and, therefore, showed no discernible emission under our experimental conditions, whereas aggregates **3** are characterized by the highest relative fluorescence quantum yield. Nonetheless, emission lifetimes of aggregate solutions under high laser fluence are 3−7 times smaller than the fluorescence decay times of aggregates **3** estimated from emission quantum yield data obtained at low light intensities. There are two possible reasons for this phenomenon: (1) aggregates **3** do not fluoresce under the conditions of the laser experiments or (2) the fluorescence lifetime of aggregates **3** in laser experiments is smaller than the lifetime estimated at low light intensities but similar to that observed under laser excitation of aggregate solutions. Both explanations assume strong quenching of aggregates **3** singlet excited state under high laser fluence. Such a strong quenching is frequently observed under intense laser excitation and originates from singlet−singlet annihilation of excited dye molecules.[31,34−36] As a result of this bimolecular annihilation of excited molecules, the emission decay kinetics are typically faster and nonexponential. The exponential profile of the emission decay of aggregate solutions illustrated in Figure 7 precludes the second explanation (2). Consequently, the observed data point to a high efficiency of singlet−singlet annihilation of excited porphyrin molecules in aggregates **3**.

It is interesting that aggregates **1** and **2** have similar (within a factor of 2; Table 2) emission quantum yields and emission lifetimes. We deduce that the observed emission decay kinetics are dominated mostly by the fluorescence decay of aggregates **1** and/or **2**. In addition, the close similarities in the emission decay lifetimes in laser experiments with those of aggregates **1** and aggregates **2** estimated from emission quantum yield data are consistent with a low efficiency for the singlet−singlet annihilation process for the excited porphyrins in either or both of these aggregates.

Thus, comparison of laser fluorescence data with fluorescence data obtained under low-excitation light intensities infers that aggregates **4** are characterized by high relative values of the nonradiative rate constant k_{nr} of excited singlet-state decay. By contrast, aggregates **3** are characterized by low relative values of k_{nr} and high efficiencies for singlet−singlet excited-state annihilation. Aggregates **1** and/or aggregates **2** are distinguished by moderate relative values of k_{nr} and by low efficiencies for the singlet−singlet excited-state annihilation process (cf. Table 4).

Time-Resolved Fluorescence Polarization Anisotropy. The amplitude of the fluorescence and the characteristic decay times of porphyrin aggregates depend on the relative orientation of the polarizing filter with respect to the orientation of the excitation light. Figure 8a shows the temporal profiles of the fluorescence from a solution of H_2TPyP aggregates for parallel ($A_{||}$) and perpendicular ($A_\perp$) orientations of the polarization filter. The origin of the phenomenon is due to rotation of porphyrin molecules and/or aggregates during the lifetime of the excited state.[67] Thus, measurements of the temporal behavior of individual polarizations of aggregates fluorescence in solution can provide an estimate of the size of the aggregates. When the time interval between excitation and emission is short, the polarization of the emission and of the incident light should practically be the same. For longer lived excited states, the orientations of the excited aggregates will be partly randomized owing to their rotation; the emitted light should then be more depolarized. The characteristic rotational relaxation time, τ_r, of the temporal profile of the polarization anisotropy, $r(t)$ (eq 5), is related to the volume V and, therefore, the size of the aggregate through Einstein's equation (eq 6)[68,69]

$$r(t) = \frac{A_{||}(t) - A_\perp(t)}{A_{||}(t) + 2A_\perp(t)} = r(0)\exp\{-t/\tau_r\} \quad (5)$$

$$\tau_r = \frac{V\eta}{\kappa T} \quad (6)$$

where ($A_{||}$) and ($A_\perp$) describe the amplitude of the fluorescence components parallel and perpendicular, respectively, to the polarization of the excitation; $r(0)$ is the polarization anisotropy at time zero; η is the viscosity of the solvent; κ is Boltzmann's constant; and T is the temperature of the surrounding solvent medium. Equation 6 presumes a spherical form for the aggregates; hence, τ_r refers to the rotational relaxation time of the spherical cluster.

Figure 8b (data points) depicts the temporal profile of the polarization anisotropy of H_2TPyP aggregates calculated from the data of Figure 8a and eq 5. The solid curve was drawn using the expression $r(t) \propto \exp\{-t/\tau_r\}$. Rotational relaxation times τ_r of different porphyrin aggregates vary between 100 and 200 ps (Table 3). These rotational times are nearly identical to the rotational relaxation time for hematoporphyrin aggregates in a phosphate buffer, $\tau_r = 100$ ps.[67]

Evaluation of the volume V of the aggregates (eq 6) necessitates knowledge of the temperature T and viscosity η of the solvent surrounding the excited porphyrin aggregate. Our earlier study[44] in the picosecond time domain showed that this temperature strongly exceeds the temperature of the bulk solvent because of thermal relaxation of the excited porphyrin aggregates. Experimental estimates analogous to those made earlier also reveal that laser light absorption heats the porphyrin aggregates from ambient temperatures to about 140 °C (note that the upper limit of the aggregate temperature is about 1000 °C [44]). With these temperatures and the viscosity of water $\eta = 0.28$ cP[70] taken as a measure of the viscosity of water surrounding the excited aggregates, together with the rotational relaxation times of Table 3, we can estimate (eq 6) the lower

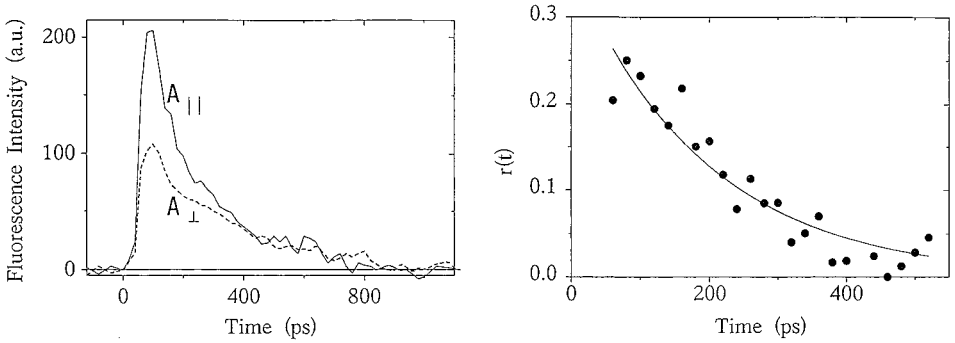

Figure 8. (a) Temporal profiles of the fluorescence of H_2TPyP aggregates solution for parallel ($A_{\parallel}$) and perpendicular ($A_{\perp}$) orientations of the polarization filter with respect to orientation of the excitation light. (b) Temporal profile of the polarization anisotropy: points, experimental data; solid line, exponential fit with $\tau_r = 190$ ps.

TABLE 4: Characteristics of Porphyrin Aggregates

porphyrin	λ_{max}, nm[a]	$10^{-9}\ k_{nr}\ s^{-1}$ [b]	relative efficiency of S—S annihilation	size, Å[c] aggregate **1**/**2**	$\Delta\nu_{abs}$, eV[d] **2**	**3**	**4**
	392	3.6	low (either or both)	16—21 (either or both)			
	423	6.4					
H_2TPP	451	1.4	high		0.07	0.25	0.36
	470	320					
	396	5.4	low (either or both)	19—27 (either or both)			
	434	6.8					
H_2TpyP	443	1.4	high		0.07	0.13	0.29
	469	200					
	392	42	low (either or both)	15—20 (either or both)			
	425	33					
H_2TPPC	442	4	high		0.01	0.13	0.24
	460	800					

[a] Maximum wavelength of Soret components. [b] Evaluation from eq 4. [c] Evaluation from eq 6. [d] Wavelength shift of aggregates.

and upper limits of the sizes D (diameters) of the porphyrin aggregates; they are collected in Table 4. Porphyrin aggregates range in size from 15 to 27 Å and contain from 3 to 20 individual porphyrin molecules. To the extent that the experimental emission decay kinetics are dominated principally by the fluorescence decay of aggregates **1** and/or **2**, the estimated aggregate size range from 15 to 27 Å must refer almost entirely to these aggregates.

The sizes of aggregates **2**, **3**, and **4** can, in principle, be estimated from the shifts of their Soret absorption maxima using the "particle-in-a-box" model frequently used to describe the optical spectral changes of semiconductor nanoparticles, i.e., molecular aggregates in which generation of charge-transfer excitons is responsible for their absorption characteristics. As with certain semiconductor nanoparticles that display demonstrated quantum size effects, J-aggregates also show the expected blue shift of their absorption spectra with a decrease in aggregate size (cf. Table 4). This model relates the shift of the excitonic band of the aggregates or nanoparticles to their sizes D[71−73]

$$\Delta\nu_{abs} = \frac{2h^2\pi^2}{\mu D^2} \qquad (7)$$

where μ is the exciton effective mass and D is the diameter of the presumed spherical cluster. Unfortunately, both the nature of the excitonic transitions in the porphyrin aggregates and the effective mass of the excitons are either unknown or experimentally unavailable,[74] thereby precluding any inferences about the sizes of the J-aggregates specifically treated in the present study. Thus, estimates of size for aggregates **3** and **4** (at least) must await further considerations.

Conclusions

Aqueous solutions of high concentrations of free base porphyrin contain aggregates whose absorption spectral features are characterized by invariant Soret band positions and by bandwidths that do not depend on the preparative procedures. The Soret band position for one type of aggregates (H-aggregate) is blue-shifted, whereas for the other aggregates (J-aggregates) it is red-shifted. The optical spectral data have been rationalized using a model which has assumed (see ref 45) the existence of four different types of porphyrin aggregates which have provided the most consistent illustration of the events under various conditions. The fluorescence quantum yields of these aggregates vary from 10^{-5} to 10^{-2}, and fluorescence emission lifetimes vary from ~1 ps to 1 ns; both properties are at least more than an order of magnitude smaller than those of the corresponding monomeric free base porphyrins. The aggregates are characterized by different rate constants of nonradiative excited singlet-state decay and different efficiencies of singlet−singlet annihilation at the high laser fluence used. Fluorescence decay lifetimes of the aggregates correlate fairly well with the corresponding characteristic times of their Soret band absorption recovery. Of particular importance is the significance of variations in the photophysical properties of dye (porphyrins, cyanines, inorganic dye antennae) monomers when they aggregate either in solutions or on solid surfaces. Such aggregations will impart different and novel photophysical properties to the dyes, a point that needs to be considered when using such dyes in certain applications. Size estimates of aggregates **1** and/or **2** have been assessed by time-resolved polarization anisotropy and lie between 15 and 27 Å; however, structural details of these aggregates in such sols continue to elude experimentation.

Acknowledgment. Support of this work by the Natural Science and Engineering Research Council (NSERC) of Canada is acknowledged. R.K. thanks the Russian Fund for Basic Research for a grant (Grant No. 96-03-32360). We are particularly grateful to NATO for Linkage Grant No. HTECH.LG 951443 (1996, 1997) between our respective laboratories. We also have appreciated the skillful technical assistance of Mr. R. Danesh during the laser experiments.

References and Notes

(1) *Bioenergetics of Photosynthesis*; Govindjee, Ed.; Academic Press: New York, 1975.

(2) Dougherty, T. J.; Kaufman, J. E.; Goldfarb, A.; Weishaupt, K. R.; Boyle, D. G.; Mittelman, M. *Cancer Res.* **1978**, *38*, 2628.

(3) Dougherty, T. J.; Thoma, R. E. In *Lasers in Photomedicine and Photobiology*; Pratesi, R., Sacchi, C. A., Eds.; Springer-Verlag: Berlin, 1980; p 67.

(4) Yamashita, M.; Nomura, M.; Kobayashi, S.; Sato, T.; Aizawa, K. *IEEE J.* **1984**, *QE−20*, 1363.

(5) Katz, J. J.; Bowman, M. K.; Michalski, T. J.; Worcester, D. L. In *Chlorophylls*; Scheer, H., Ed.; CRC Press: Boca Raton, FL, 1991; pp 211−235.

(6) Scheer, H.; Katz, J. J. In *Porphyrins and Metalloporphyrins*; Smith, K. M., Ed.; Elsevier: Amsterdam, 1975; p 393.

(7) White, W. I. In *The Porphyrins*; Dolphin, D., Ed.; Academic: New York 1978; Vol. 5, p 303.

(8) Barber, D. C.; Freitag, R. A.; Whitten, D. G. *J. Phys. Chem.* **1991**, *95*, 4074.

(9) Pashenko, V. Z.; Protasov, S. P.; Rubin, A. B.; Timofeev, K. N.; Zamazova, L. M.; Rubin, L. B. *Biochim. Biophys. Acta* **1975**, *408*, 145.

(10) Campillo, A. J.; Shapiro, S. L. In *Ultrafast Light Pulses*; Shapiro, S. L., Ed.; Springer: Berlin, 1977; Chapter 7.

(11) Meech, S. R.; Stubbs, C. D.; Phillips, D. *IEEE J.* **1984**, *QE−20*, 1343.

(12) Tail, C. D.; Holten, D.; Gouterman M. *Chem Phys. Lett.* **1983**, *100*, 268.

(13) Bergkamp, M. A.; Dalton, J.; Netzel, T. L. *J. Am. Chem. Soc.* **1982**, *104*, 253.

(14) Chen, J.-T.; Yu, Z.-X. *Appl. Phys. B* **1990**, *50*, 313.

(15) Butvilas, V.; Gulbinas, V.; Urbas, A. *Inst. Phys. Conf. Ser.* **1991**, *126*, 503.

(16) Causgrove, T. P.; Cheng, P.; Brune, D. C.; Blankenship, R. E. *J. Phys. Chem.* **1993**, *97*, 5519.

(17) Pasternack, R. F.; Huber, P. R.; Boyd, P.; Engasser, G.; Francesconi, L.; Gibbs, E.; Fasella, P.; Cerio Venturo, G.; Hinds, L. C. *J. Am. Chem. Soc.* **1972**, *94*, 4511.

(18) Das, R. R. *J. Inorg. Nucl. Chem.* **1975**, *37*, 153.

(19) Ojadi, E.; Selzer, R.; Linschitz, H. *J. Am. Chem. Soc.* **1985**, *107*, 7783.

(20) van Willigen, H.; Chandrasekar, T. K.; Das, U.; Ebersole, M. H. In *Porphyrins: Excited States and Dynamics*; Gouterman, M., Rentzepis, P. M., Straub, K. D., Eds.; ACS Symposium Series 321; American Chemical Society: Washington, DC, 1986; pp 140−153.

(21) Gibbs, E. J.; Tinaco, I., Jr.; Maestre, M. F.; Ellinas, P. A.; Pasternack, R. F. *Biochim. Biophys. Res. Commun.* **1988**, *157*, 350.

(22) Hunter, C. A.; Sanders, J. K. M. *J. Am. Chem. Soc.* **1991**, *95*, 4074.

(23) Knox, R. S. In *Bioenergetics of Photosynthesis*; Govindjee, Ed.; Academic: New York, 1975, p 183.

(24) Seely, G. R.; Connolly, J. S. In *Light Emission by Plants and Bacteria*; Govindjee, Amesz, J., Fork, D. C., Eds.; Academic Press: Orlando, 1986; pp 99−133.

(25) Brookfield, R. L. In *Primary Photoprocesses in Biology and Medicine*; Bensasson, R. V., Ed.; Plenum: New York, 1985; p 329.

(26) Andereori, A.; Cubeddu, R.; De Silvestry, S.; Laporta, P.; Jori, G.; Reddi, E. *Chem. Phys. Lett.* **1984**, *108*, 141.

(27) Yamashita, M.; Nomura, M.; Kobayashi, S.; Sato, T.; Aizawa, K. *IEEE J.* **1984**, *QE−20*, 1363.

(28) Sha, W.-L.; Chen, J.-T.; Yu, Z.-X.; Liu, S.-H. In *Laser Materials and Laser Spectroscopy*; Wang, Z. J., Ed.; World Scientific: Singapore, 1989; p 253.

(29) Hall, R. S.; Oh, Y. S.; Johnson, C.S. *J. Phys. Chem.* **1980**, *84*, 756.

(30) Levanon, H.; Vega, S. *J. Chem. Phys.* **1974**, *61*, 2265.

(31) Breton, J.; Geacintov, N. E. *Biochim. Biophys. Acta* **1980**, *594*, 1.

(32) Van Grondelle, R. *Biochim. Biophys. Acta* **1985**, *811*, 147.

(33) Van Grondelle, R. *Biochim. Biophys. Acta* **1985**, *811*, 17.

(34) Campilo, A. J.; Shapiro, S. L. *Photochem. Photobiol.* **1978**, *28*, 975.

(35) Swenberg, C. E.; Geacintov, N. E.; Breton, J. *Photochem. Photobiol.* **1978**, *28*, 999.

(36) Pallotin, G.; Swenberg, C. E.; Breton, J.; Geacintov, N. E. *Biophys. J.* **1979**, *25*, 513.

(37) In *Theory of Photographic Processes*, 4th ed.; James, T. H., Ed., Macmillan: New York, 1977.

(38) Wang, N.; Chernyak, V.; Mukamel, S. *J. Chem. Phys.* **1994**, *100*, 2465.

(39) Wang, N.; Jenkins, J. K.; Chernyak, V.; Mukamel, S. *Phys. Rev. B* **1994**, *49*, 17079.

(40) Wang, N.; Mukamel, S. *Chem. Phys. Lett.* **1994**, *231*, 373.

(41) Wang, N.; Rabitz, H. *J. Phys. Chem.* **1995**, *99*, 6789

(42) Bawendi, M. C.; Steigerwald, M. L.; Brus, L. E. *Annu. Rev. Phys. Chem.* **1990**, *41*, 477.

(43) (a) Gratzel, M.; Kalyanasundaram, K. In *Photosensitization and Photocatalysis Using Inorganic and Organometallic Compounds*; Kalyanasundaram, K., Gratzel, M., Eds.; Kluwer Academic Publishers: Dordrecht, 1993; p 247. (b) Miller, R. J. D.; McLendon, G. L.; Nozik, A. J.; Schmickler, W.; Willig, F. *Surface Electron Transfer Processes*; VCH: New York, 1995; p 370.

(44) Khairutdinov, R. F.; Serpone, N. *J. Phys. Chem.* **1995**, *99*, 11952.

(45) Although a model based on five-component deconvolution would yield a better fit ($r^2 = 0.99995$) to free base porhyrin aggregates absorption spectra than a four-component deconvolution ($r^2 = 0.99984$), a five-component (or higher) aggregates solution does not yield a reasonable fit to the wavelength dependence of the emission quantum yield data illustrated in Figure 4 (experimental points).

(46) Serpone, N.; Sharma, D. K.; Moser, J.; Gratzel, M. *Chem. Phys. Lett.* **1987**, *136*, 47.

(47) Serpone, N.; Sharma, D. K.; Jamieson, M. A.; Gratzel, M.; Ramsden, J. J. *Chem. Phys. Lett.* **1985**, *115*, 473.

(48) Moser, J.; Gratzel, M.; Sharma, D. K.; Serpone, N. *Helv. Chim. Acta* **1985**, *68*, 1686.

(49) Yu, W. In *Picosecond Phenomena*; Shank, C. V., Ippen, E. P., Shapiro, S. L., Eds.; Springer: Berlin, 1978; p 3466ff.

(50) Uehara, K.; Hioko, Y.; Mimuro, M. *Photochem. Photobiol.* **1993**, *58*, 127

(51) Tail, C. D.; Holten, D.; Gouterman, M. *Chem. Phys. Lett.* **1983**, *100*, 268.

(52) West, W.; Pearce, S. *J. Phys. Chem.* **1965**, *69*, 1894.

(53) Dewey, T. G.; Raymond, D. A.; Turner, D. H. *J. Am. Chem. Soc.* **1979**, *101*, 5822.

(54) Kano, K.; Nakajima, T.; Hashimoto, S. *J. Phys. Chem.* **1987**, *91*, 6614.

(55) Stone, A. L.; Fleisher, E. B. *J. Am. Chem. Soc.* **1968**, *90*, 2744.

(56) Wasielewski, M. R.; Niemczyk, M. P.; Sveck, W. A. *Tetrahedron Lett.* **1982**, *23*, 3215.

(57) Chang, C. K. *Adv. Chem. Ser.* **1979**, *173*, 162.

(58) Gibbs, E. J.; Tinaco, I., Jr.; Maestre, M. F.; Ellinas, P. A.; Pasternack, R. F. *Biochem. Biophys. Res. Commun.* **1988**, *157*, 350.

(59) Kasha, M. *Radiat. Res.* **1963**, *20*, 55.

(60) Chang, C. K. *J. Heterocycl. Chem.* **1977**, *14*, 1285.

(61) Hochstrasser, R. M.; Kasha, M. *Photochem. Photobiol.* **1964**, *3*, 317.

(62) Davydov, A. S. *Theory of Molecular Excitons*; McGraw-Hill: New York, 1962.

(63) Bird, G. R.; Norland, K. S.; Rosenoff, A. E.; Michaud, H. B. *Photograph. Sci. Eng.* **1968**, *12*, 196.

(64) Gouterman, M. In *The Porphyrins*; Dolphin, D., Ed.; Academic: New York, 1978; Vol. 3, pp 1−165.

(65) Rodriguez, J.; Kirmaier, C.; Holten, D. *J. Am. Chem. Soc.* **1989**, *111*, 6500.

(66) Akins, D. L.; Zhu, H.-R.; Guo, C. *J. Phys. Chem.* **1996**, *100*, 5420.

(67) Vardanyan, A. G.; Kamalov, V. E.; Mironov, A. F.; Struganova, I. A.; Toleutaev, B. N. *Opt. Spectrosc.* **1989**, *66*, 199.

(68) Einstein, A. *Investigation on the Theory of the Brownian Movement*; Dover Publications: New York, 1956.

(69) O'Connor, D. V.; Phillips, D. *Time-Correlated Single Photon Counting*; Academic Press: London, 1984; pp 252−283.

(70) The value $\eta = 0.28$ corresponds to the viscosity of water at 100 °C (*Handbook of Chemistry and Physics*, 51st ed.; Weast, R. C., Ed.; The Chemical Rubber Co: Clevland, 1970; p F36). This is an upper limit of the viscosity of the solvent medium around aggregates heated to $T > 100$ °C.

(71) Efros, Al. L.; Efros, A. L. *Sov. Phys. Semicond.* **1982**, *16*, 772.

(72) Brus, L. E. *J. Chem. Phys.* **1984**, *80*, 4403.

(73) Steierwald, M. L.; Brus, L. E. *Acc. Chem. Res.* **1990**, *23*, 183.

(74) Meier, H. *Dark and Photoconductivity of Organic Solids*; Verlag Chemie GmbH: Weinheim, 1974; p 46.